FLIGHT TRAJECTORY CONTROL BASED ON REQUIRED ACCELERATION FOR FIXED-WING AIRCRAFT

Naoharu Yoshitani
Dept. of Aerospace Engineering, Teikyo University, Utsunomiya, Japan

Keywords: *flight dynamics, trajectory control, acceleration vector, flight simulation*

Abstract

This paper presents an automatic trajectory control of a fixed-wing aircraft. In the control, a desired flight trajectory is first determined as a sequence of segments of line, circle and helix smoothly connected in the three-dimensional space. A unit vector of direction command is then obtained so that the aircraft flies smoothly along the desired trajectory. The direction deviation vector, which is orthogonal to the velocity vector, is calculated based on spherical geometry, where the algorithm has been improved from the author's previous papers. Next, a required acceleration vector of the aircraft is calculated with Proportional, Integral and Differential (PID) control scheme. In order to achieve the required acceleration, desired roll, pitch and yaw rate commands are obtained, again with PID control scheme, and are put into attitude control. The attitude controller can employ any existing control technology suitable for the aircraft to be controlled.

Thus, the proposed control does not require detailed information on aircraft dynamics and aerodynamic coefficients. This makes the proposed control relatively simple and easy to implement. Numerical simulations illustrate the effectiveness of the control.

Nomenclature

$\{I\}$ frame : NED (North, East, Down) inertial frame
$\{B\}$ frame : body frame fixed to the aircraft
$\{S\}$ frame : stability frame
$\{W\}$ frame : wind frame
$\{V\}$ frame : 'velocity frame', obtained by rotating the wind frame about the x-axis so that the y-axis becomes horizontal.
$\{V_{y(-z)}\}$ plane : the plane defined by the y and $(-z)$-axes of $\{V\}$ frame, perpendicular to the velocity
$x_B, y_B, z_B; x_S, y_S, z_S; x_W, y_W, z_W; x_V, y_V, z_V$: x, y, z axes of $\{B\}$, $\{S\}$, $\{W\}$ and $\{V\}$ frame, respectively
ϕ, θ, ψ : Euler angles (roll, pitch, yaw)
p, q, r : roll, pitch and yaw rate
α, β : angle of attack, side-slip angle
ϕ_b : bank angle (around the x axis of $\{S\}$ frame)
λ : heading angle, where the north and the east are expressed by 0 and $(\pi/2)$ [rad], respectively
γ : flight-path angle (climb angle)
$\vec{g}$: gravity vector; g denotes $\|\vec{g}\|$.
$\vec{V}_a$: velocity vector of the aircraft
$\boldsymbol{\zeta}$: aircraft position in $\{I\}$ frame
$\vec{\xi}$: a unit vector of aircraft direction
$\vec{a}_c$: required acceleration vector in $\{V_{y(-z)}\}$ plane
$\{\cdot\}_c$: command of a variable
$\{\cdot\}^T$: transposed vector or matrix
$(\cdot \ \cdot)^T_{Vy(-z)}$: a vector in $\{V_{y(-z)}\}$ plane expressed by the y_V and $(-z_V)$ coordinates
Δt : control interval except attitude and velocity control

Fig. 1 shows a fixed-wing aircraft with $\{B\}$ frame.

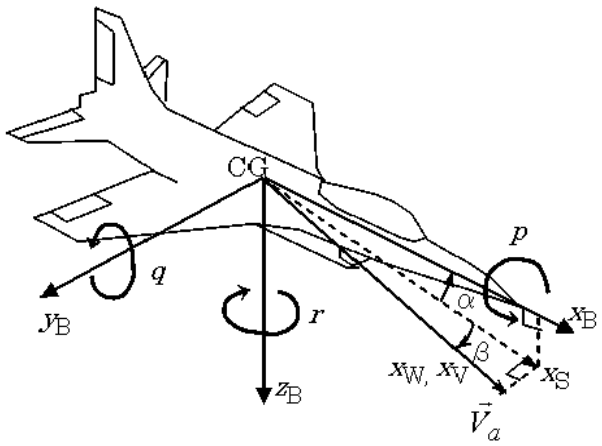

Fig. 1 Fixed-Wing Aircraft with $\{B\}$ Frame

1 Introduction

Automatic control of flight trajectory is indispensable for operating Unmanned Aerial Vehicles (UAVs) and for relieving human pilots of work loads. A number of control algorithms have been proposed to control an aircraft automatically along its desired trajectory [1]-[8]. These algorithms require the dynamic model of the aircraft with aerodynamic coefficients to obtain control input values such as deflections of control surfaces.

In this paper, an algorithm of flight trajectory control is described for a fixed-wing aircraft. The algorithm has been improved to be more efficient than that in the author's previous papers [9, 10]. The control is based on a required acceleration vector, which is perpendicular to the velocity vector of the aircraft. Some other studies [4, 6] also introduce a required (or desired) acceleration or force, which is defined in $\{I\}$ frame and is used to move the center of gravity (CG) of the aircraft toward the desired direction.

Unlike this, a required acceleration $\vec{a}_c$ in the proposed control is defined as a vector in $\{V_{y(-z)}\}$ plane, perpendicular to the velocity. $\vec{a}_c$ is used to control the direction and the curvature of the aircraft trajectory. A large direction deviation leads to a $\vec{a}_c$ of large norm to change the direction quickly, which is not the case in other studies.

The control objective is to achieve the following C1 to C3.

C1 The aircraft position is on the desired trajectory.
C2 The aircraft flying direction is along the desired trajectory.
C3 The aircraft trajectory has the same curvature as the desired trajectory.

C1 to C3 are necessary to keep the aircraft flying along the desired trajectory.

The followings are the features and advantages of the proposed control compared with those of other studies:

A1 The required acceleration vector is perpendicular to the velocity. It is obtained mainly from the direction of the actual velocity $\vec{V}_a$ and its command $\vec{V}_{ac}$. This enables to change the velocity direction quickly when there is a large direction deviation.
A2 In order to prevent excessive rolling movement, the bank angle command is appropriately determined as $\angle(\vec{a}_{cg})$ or $[\angle(\vec{a}_{cg})+\pi]$, where $\angle(\vec{\cdot})$ is the angle of a vector and $\vec{a}_{cg}$ is a required acceleration including gravity cancellation.
A3 Feedback control is based on well-established PID control, where the inverse dynamics and aerodynamic coefficients of the aircraft are not required in control design nor in online calculation.
A4 The curvature of the flight trajectory is controlled by feedforward control to keep the aircraft close to the desired trajectory.
A5 The attitude control can employ any control algorithm, PID or more sophisticated one. This enables to implement the proposed control without much modification in the existing control system of the aircraft, and makes the algorithm reliable and easy to apply.

The above A1 to A3 are hardly found in other studies on trajectory control. The proposed control is best suitable for highly maneuverable aircraft such as fighter planes and, by placing limits on acceleration, angles or angular rates, it can be applied to other types of aircraft.

2 Control Algorithm

Fig. 2 shows the proposed control system. The input to the system is a desired trajectory T_{rc}, which is required to be smooth, i.e., the first derivative of the trajectory is continuous without any jumps.

Considering this, a desired trajectory is determined as a sequence of segments of line, circle and helix, smoothly connected together. When the desired trajectory is beyond the flight capability of the aircraft, or when sudden disturbances break out, it is inevitable that the aircraft would go off the desired trajectory. Even in this situation, the aircraft would eventually come back to the desired trajectory with the proposed control, as shown later in simulation results.

The control system is hierarchical and multi-cascaded. The algorithm at each controller will be described in this section.

2.1 Trajectory Controller

This controller calculates a unit direction command vector $\vec{\xi}_{\mathrm{c}}$ to satisfy C1 to C3 described in Section 1. When the aircraft is well away from the desired trajectory, C1 is given priority. When the aircraft comes close to the desired trajectory, C2 and C3 are given priority. The detailed algorithm will be described step by step.

2.1.1 Direction Command Vector $\vec{\xi}_{\mathrm{c}}$

Fig. 3 shows an example of actual and desired trajectory. At each control instance, the controller finds out 'reference point' $\boldsymbol{\zeta}_{\mathrm{ref}}$ on the desired trajectory, where $\boldsymbol{\zeta}_{\mathrm{ref}}$ is the nearest point to the aircraft in the forward section from $\boldsymbol{\zeta}_{\mathrm{ref}(-1)}$, which is the reference point at the previous control instance. Thus, $\boldsymbol{\zeta}_{\mathrm{ref}}$ does not move back on the desired trajectory. Let $\vec{\xi}_{\mathrm{ref}}$ denote the unit vector along the desired trajectory at $\boldsymbol{\zeta}_{\mathrm{ref}}$.

On the desired trajectory, let 'aimed point' and 'FF point', denoted by $\boldsymbol{\zeta}_{\mathrm{aim}}$ and $\boldsymbol{\zeta}_{\mathrm{FF}}$, be defined as the point located forward from $\boldsymbol{\zeta}_{\mathrm{ref}}$ by the distance of d_{aim} and d_{ff}, respectively, where d_{aim} and d_{ff} are defined by

$$d_{\mathrm{aim}} = \max\{t_{\mathrm{aim}}V_{\mathrm{a}},\ r_{\mathrm{e}_\zeta}e_\zeta\} \quad (1)$$

$$d_{\mathrm{ff}} = t_{\mathrm{ff}}V_{\mathrm{a}} \quad (2)$$

$$\text{where } e_\zeta = \|\boldsymbol{\zeta}_{\mathrm{ref}} - \boldsymbol{\zeta}\| \quad (3)$$

Here, e_ζ represents the position deviation. t_{aim} [s], r_{e_ζ} and t_{ff} [s] are design parameters, where smaller values should be set when the aircraft has high ability to maneuver and the control response is required to be as quick as possible. d_{aim} can be either smaller or larger than d_{ff} and the figure shows the case of $d_{\mathrm{aim}} > d_{\mathrm{ff}}$. When $e_\zeta < (t_{\mathrm{aim}}V_{\mathrm{a}}/r_{\mathrm{e}_\zeta})$ in (1), $\boldsymbol{\zeta}_{\mathrm{aim}}$ is t_{aim} seconds away from $\boldsymbol{\zeta}_{\mathrm{ref}}$. In other situations, the distance from $\boldsymbol{\zeta}_{\mathrm{ref}}$ to $\boldsymbol{\zeta}_{\mathrm{aim}}$ is proportional to e_ζ.

Further, let 'desired direction' of the aircraft be defined as the direction to $\boldsymbol{\zeta}_{\mathrm{aim}}$ from the aircraft, and let $\vec{\xi}_{\mathrm{aim}}$ denote the unit vector in this direction. Let 'desired curvature' of the aircraft be defined as the curvature of the desired trajectory at $\boldsymbol{\zeta}_{\mathrm{FF}}$. Let $\vec{\xi}$ and $\vec{\xi}_{\mathrm{c}}$ denote the unit velocity vector and its command. $\vec{\xi}_{\mathrm{c}}$ is defined by

$$\vec{\xi}_{\mathrm{c}} = w_{\mathrm{aim}}\vec{\xi}_{\mathrm{aim}} + (1 - w_{\mathrm{aim}})\vec{\xi}_{\mathrm{ref}} \quad (4)$$

$$\text{where } w_{\mathrm{aim}} = e_\zeta/(t_{\mathrm{e}_\zeta}V_{\mathrm{a}}),\ 0 \le w_{\mathrm{aim}} \le 1 \quad (5)$$

and where t_{e_ζ} [s] is a design parameter and w_{aim} is limited within the range $[0,\ 1]$. The first term in the right-hand side of (4) is the command for C1 in Section 1, while the second term is for C2. w_{aim} represents the weight for C1. When $e_\zeta \ge t_{\mathrm{e}_\zeta}V_{\mathrm{a}}$, $w_{\mathrm{aim}} = 1$ and C2 is not considered and, as shown later in (10), C3 is not considered either.

By using $\vec{\xi}_{\mathrm{c}}$ obtained by (4), the actual trajectory would smoothly converge to the desired one.

2.1.2 Direction Deviation

Fig. 4 shows a unit sphere in $\{V\}$ frame. Arcs on the sphere are segments of great circles.

Let $\vec{e}_\xi$ be defined as the direction deviation vector contained in $\{V_{\mathrm{y}(-\mathrm{z})}\}$ plane. It represents the difference between $\vec{\xi}$ and $\vec{\xi}_{\mathrm{c}}$. Its magnitude and angle are represented, respectively, by

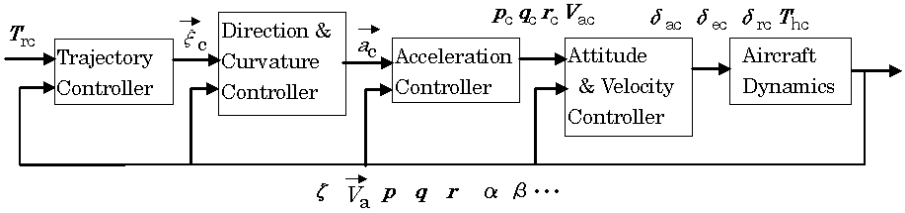

Fig. 2 Block Diagram of the Proposed Control

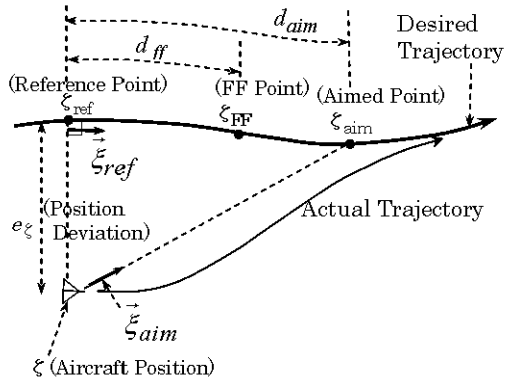

Fig. 3 Example of Actual and Desired Trajectory

$\angle$XOC, denoted by e_ξ ($\in [0,\ \pi]$), and $\angle$YXC, denoted by η_ξ. It is expressed with $y_V(-z_V)$ components as

$$\vec{e}_\xi = [e_\xi \cos\eta_\xi \quad e_\xi \sin\eta_\xi]^T_{Vy(-z)} \tag{6}$$

The algorithm to obtain $\vec{e}_\xi$ is described below. It is an improved one from the author's previous papers [9, 10].

Let $\vec{\xi}_c$ in $\{V\}$ frame be represented as $[\xi_{cx_V}\ \ \xi_{cy_V}\ \ \xi_{cz_V}]^T_V$. When $\xi_{cy_V} \neq 0$ or $\xi_{cz_V} \neq 0$, e_ξ and η_ξ are expressed by

$$2\sin\frac{e_\xi}{2} = \|\vec{\xi}_c - \vec{\xi}\| \tag{7}$$

$$\sin\eta_\xi = -\frac{\xi_{cz_V}}{\sqrt{\xi^2_{cy_V} + \xi^2_{cz_V}}} \tag{8}$$

$$\text{where} \quad \text{sign}\left\{\frac{\pi}{2} - |\eta_\xi|\right\} = \text{sign}\{\xi_{cy_V}\} \tag{9}$$

Eqn. (7) is derived by noting that the length $\overline{XC}$ is equal to $\|\vec{\xi}_c - \vec{\xi}\|$, and eqn. (8) is derived by considering the orthogonal projection of $\vec{\xi}_c$ onto the YOZ plane [11], which contains the y and z-axes of $\{V\}$ frame,

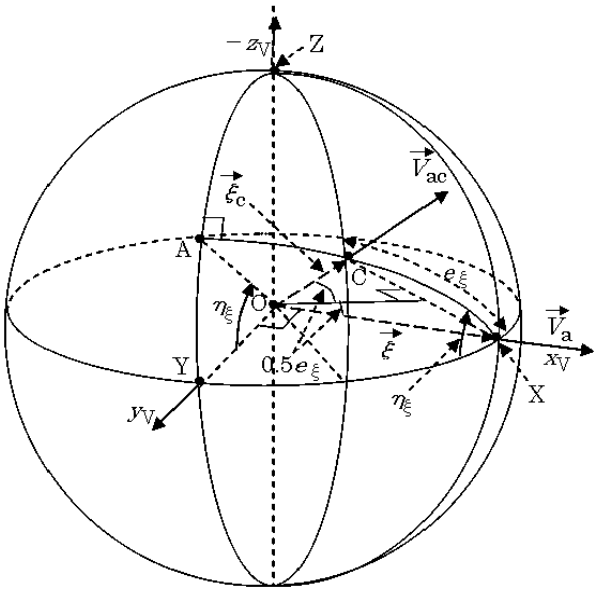

Fig. 4 Direction Deviation in $\{V\}$ Frame

When $\xi_{cy_V} = \xi_{cz_V} = 0$, any value of η_ξ is allowed and, in order to minimize the attitude fluctuation, it is kept unchanged from the value at the previous control instance.

2.2 Direction and Curvature Controller

In this controller, a required acceleration vector $\vec{a}_c$ is obtained to control the aircraft direction $\vec{\xi}$ and its trajectory curvature. $\vec{a}_c$ is the sum of a feedforward acceleration $\vec{a}_{ff}$ and a feedback acceleration $\vec{a}_{fb}$. These are contained in $\{V_{y(-z)}\}$ plane and are used for curvature control and direction control, respectively.

2.2.1 Feedforward Acceleration $\vec{a}_{ff}$

Let $\vec{\xi}_{ff}$ denote a unit vector along the desired trajectory at ζ_{ff} shown in Fig. 3. The rate of change

of $\vec{\xi}_{\mathrm{ff}}$, denoted by $\dot{\vec{\xi}}_{\mathrm{ff}}$, is orthogonal to $\vec{\xi}_{\mathrm{ff}}$. Let $\dot{\vec{\xi}}_{\mathrm{ffV}}$ denote the orthogonal projection of $\dot{\vec{\xi}}_{\mathrm{ff}}$ onto $\{V_{\mathrm{y}(-\mathrm{z})}\}$ plane. Notice that $\dot{\vec{\xi}}_{\mathrm{ff}}$ is contained in $\{V_{\mathrm{y}(-\mathrm{z})}\}$ plane when $\vec{\xi}_{\mathrm{ff}} = \vec{\xi}$.

When e_ζ or e_ξ is large, C3 in Section 1 is not given priority and $\|\vec{a}_{\mathrm{ff}}\|$ should be small. Considering this, $\vec{a}_{\mathrm{ff}}$ is given by

$$\vec{a}_{\mathrm{ff}} = V_{\mathrm{a}}(1 - w_{\mathrm{aim}}) \max\{0,\ \cos e_\xi\} \dot{\vec{\xi}}_{\mathrm{ffV}} \tag{10}$$

2.2.2 *Feedback Acceleration $\vec{a}_{\mathrm{fb}}$*

$\vec{a}_{\mathrm{fb}}$ is obtained as the manipulated variable of PID control by the following equation:

$$\vec{a}_{\mathrm{fb}} = V_{\mathrm{a}}(K_{\mathrm{aP}} \cdot \vec{e}_\xi + K_{\mathrm{aI}} \cdot \vec{S}_{\mathrm{e}_\xi} + K_{\mathrm{aD}} \cdot \dot{\vec{e}}_\xi) \tag{11}$$

In the above, K_{aP}, K_{aI} and K_{aD} are PID control gains. $\vec{S}_{\mathrm{e}_\xi}$ is the sum of the time series (integral) of $\vec{e}_\xi$, while $\dot{\vec{e}}_\xi$ is the derivative of $\vec{e}_\xi$.

Next, the procedure to update $\vec{S}_{\mathrm{e}_\xi}$ will be described. Let Δt denote the control interval and $\Delta\lambda$ and $\Delta\gamma$ denote the changes of λ and γ in the time length of Δt. Fig. 5 shows a unit sphere with the x_{V}-axis. Point $\mathrm{X}_{(-1)}$ is the Point X at Δt time before. When $\Delta\lambda, \gamma \neq 0$, $\{V_{\mathrm{y}(-\mathrm{z})}\}$ plane not only moves but also rotates about the x_{V}-axis on the sphere in Fig. 5. When $\Delta\lambda$ and $\Delta\gamma$ are both small, this rotation angle is approximated by $\Delta\eta$ in the figure, and the length of the arc $\widehat{\mathrm{PX}}$ in the figure is expressed by

$$\widehat{\mathrm{PX}} = \overline{\mathrm{SX}}\Delta\lambda \simeq \overline{\mathrm{RX}}\Delta\eta \tag{12}$$

$$\text{where} \quad \overline{\mathrm{RX}} = \frac{\overline{\mathrm{OX}}}{\tan\gamma} = \frac{\overline{\mathrm{OX}} \cdot \cos\gamma}{\sin\gamma} \tag{13}$$

$$\overline{\mathrm{OX}} = 1, \quad \overline{\mathrm{SX}} = \cos\gamma \tag{14}$$

The above equations lead to the following expression.

$$\Delta\eta \simeq \begin{cases} -\Delta\lambda \cdot \sin\gamma & (|\gamma| < |\gamma - \Delta\gamma|) \\ -\Delta\lambda \cdot \sin(\gamma - \Delta\gamma) & (\text{otherwise}) \end{cases} \tag{15}$$

Let $\vec{S}_{\mathrm{e}_\xi(-1)}$ denote $\vec{S}_{\mathrm{e}_\xi}$ at Δt time before. Its update should be done by using a coordinate rotation matrix $R_{\mathrm{V}}(\Delta\eta)$ as

$$\vec{S}_{\mathrm{e}_\xi} = \vec{e}_\xi \cdot \Delta t + R_{\mathrm{V}}(\Delta\eta)\vec{S}_{\mathrm{e}_\xi(-1)} \tag{16}$$

$$\text{where} \quad R_{\mathrm{V}}(\Delta\eta) = \begin{bmatrix} \cos\Delta\eta & -\sin\Delta\eta \\ \sin\Delta\eta & \cos\Delta\eta \end{bmatrix} \tag{17}$$

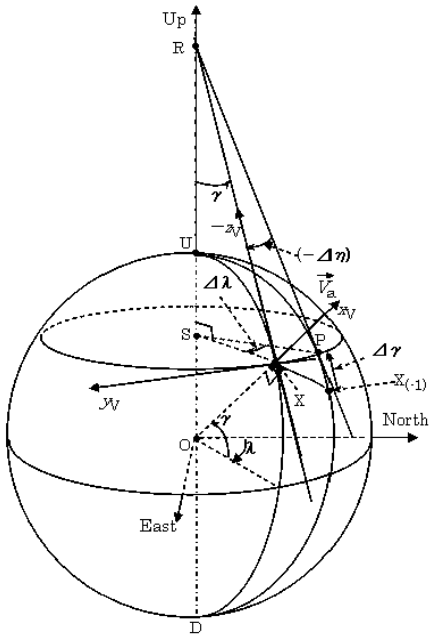

Fig. 5 Rotation Angle during Δt

2.3 Acceleration Controller

2.3.1 *Bank Angle ϕ_{b} and Its Command ϕ_{bc}*

ϕ_{b} about the x_{S}-axis represents the lift direction. ϕ_{b} can be approximated by the roll angle ϕ when $|\alpha|$ and $|\theta|$ are both small. In other situations, ϕ_{b} is accurately obtained from an equation of ϕ_{b}, ϕ, θ and α. The equation can be derived by using frame transformation matrices [12]. Its details are omitted here.

Next, the procedure to obtain the bank angle command ϕ_{bc} will be described. In the proposed control, the side-slip angle β should be controlled to zero in the attitude controller. Hence, $|\beta|$ can be considered to be small. In this situation, $\{W\}$ frame and $\{V_{\mathrm{y}(-\mathrm{z})}\}$ plane are roughly identical to $\{S\}$ frame and its yz-plane, respectively.

Let $\vec{g}_{\mathrm{V}}$ denote the orthogonal projection of the gravity acceleration vector $\vec{g}$ onto $\{V_{\mathrm{y}(-\mathrm{z})}\}$ plane. Let $\vec{a}_{\mathrm{cg}}$ represent the required acceleration including gravity cancellation, given by

$$\vec{a}_{\mathrm{cg}} = \vec{a}_{\mathrm{c}} - \vec{g}_{\mathrm{V}} \tag{18}$$

$$\text{where} \quad \vec{g}_{\mathrm{V}} = [0 \quad -g\cos\gamma]^{\mathrm{T}}_{\mathrm{Vy}(-\mathrm{z})} \tag{19}$$

Let $\angle^{(-z_{\mathrm{V}})}(\vec{a}_{\mathrm{cg}})$ denote the angle of $\vec{a}_{\mathrm{cg}}$ from the $(-z_{\mathrm{V}})$-axis, and let $e_{a\phi}(\in [-\pi, \pi])$ denote the an-

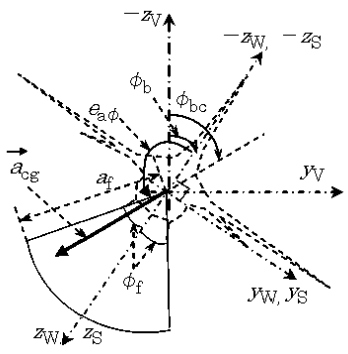

Fig. 6 Bank Angle ϕ_b and Its Command ϕ_{bc}

gle $[\angle^{(-z_V)}(\vec{a}_{cg}) - \phi_b]$. Fig. 6 shows ϕ_b, its command ϕ_{bc} and related angles in the *yz*-plane of $\{S\}$, $\{V\}$ and $\{W\}$ frames.

A main aerodynamic force vector contained in this plane is a lift, which is required to be in the direction of $\vec{a}_{cg}$. Thus, ϕ_{bc} is required to be $\angle^{(-z_V)}(\vec{a}_{cg})$ or $[\angle^{(-z_V)}(\vec{a}_{cg}) + \pi]$ [rad], depending on the value of $e_{a\phi}$ and $\|\vec{a}_{cg}\|$. When $|e_{a\phi}|$ is larger than $(\pi - \phi_f)$ [rad] and $\|\vec{a}_{cg}\|$ is less than a_f, as shown in Fig. 6, ϕ_{bc} is set at $[\angle^{(-z_V)}(\vec{a}_{cg}) + \pi]$ [rad] to prevent excessive rolling movement. Here, ϕ_f and a_f are design parameters. Thus, ϕ_{bc} is given by

$$\phi_{bc} = \begin{cases} \angle^{(-z_V)}(\vec{a}_{cg}) + \pi \ \text{[rad]} \\ \quad (|e_{a\phi}| > \pi - \phi_f \ \& \ \|\vec{a}_{cg}\| < a_f) \\ \angle^{(-z_V)}(\vec{a}_{cg}) \ \text{[rad]} \quad (\text{otherwise}) \end{cases} \tag{20}$$

2.3.2 *Angular Rate Commands p_c and q_c*

The roll rate command p_c is used as the manipulated variable to control the bank angle ϕ_b to ϕ_{bc}. It is given by

$$p_c = K_{pP} \cdot (\phi_{bc} - \phi_b) \tag{21}$$

K_{pP} is a control gain. When $(\phi_{bc} - \phi_b)$ goes beyond the range $[-\pi, \ \pi]$, 2π or -2π is added to it to keep its value within the range.

Regarding the pitch rate command q_c, let a_{cL} denote the $(-z_W)$ component of $\vec{a}_c$. It is given by

$$a_{cL} = \|\vec{a}_c\| \cos(\phi_b - \angle^{(-z_V)}(\vec{a}_c)) \tag{22}$$

On the other hand, if we regard q_c as the pitch rate required to generate a_{cL}, a_{cL} is expressed by

$$a_{cL} = V_a \cdot (q_c - \dot{\alpha}) \tag{23}$$

when $|\beta|$ is small. From (22) and (23), q_c is obtained. In calculating q_c, it may be better to omit $\dot{\alpha}$ in (23) if the control tends to deteriorate to be oscillatory.

2.3.3 *Limits of α and G-force a_{z_B}*

These values should be limited within appropriate ranges: $[\alpha_{max}, \ \alpha_{min}]$ and $[a_{z_B max}, \ a_{z_B min}]$, respectively, where a_{z_B} denotes the z_B-axis component of the aircraft acceleration. These ranges are determined by considering the safety for humans and for the aircraft, and the limits of flight capability. α and a_{z_B} are limited within the appropriate range by limiting q_c.

First, how to limit α roughly under α_{max} is described. Let $q_{cmax\alpha}$ be the manipulated variable to control α to α_{max} when $(\alpha_{max} - \alpha) \leq \Delta\alpha$, where $\Delta\alpha$ is a small positive constant. When $(\alpha_{max} - \alpha) \leq \Delta\alpha$, $q_{cmax\alpha}$ is updated as

$$\begin{aligned} q_{cmax\alpha} \ = \ & q_{c(-1)} - K_{\alpha P} \cdot \dot{\alpha} \cdot \Delta t \\ & + K_{\alpha I} \cdot (\alpha_{max} - \alpha) \cdot \Delta t \end{aligned} \tag{24}$$

$q_{c(-1)}$ is the value of q_c at the previous control instance. $K_{\alpha P}$ and $K_{\alpha I}$ are PI control gains. When $(\alpha_{max} - \alpha) > \Delta\alpha$, $q_{cmax\alpha}$ is not calculated.

Next, when $|\beta|$ is small, a_{z_B} is expressed by

$$a_{z_B} = g \cos\theta \cdot \cos\phi + V_a \cdot (q - \dot{\alpha}) \cos\alpha \tag{25}$$

The value of q_{cmaxz} to limit a_{z_B} roughly under $a_{z_B max}$ is obtained from (25) by replacing a_{z_B} and q with $a_{z_B max}$ and q_{cmaxz}, respectively, where $\dot{\alpha}$ can be omitted. The upper limit of q_c is set at $\min\{q_{cmax\alpha}, \ q_{cmaxz}\}$. The lower limit of q_c is obtained similarly.

2.4 Attitude and Velocity Controller

For the control of p, q, r and V_a, any suitable control law such as PID control can be applied. Typical manipulated variables for these are commands to ailerons, elevator, rudder and engine thrust, respectively, for a conventional fixed-wing aircraft.

3 Numerical Simulation

The algorithm described so far has been tested to control an F-16 fighter plane through computer simulations. The simulation software was developed under MATLAB/SIMULINK environment. The nonlinear six DOF (degree of freedom) dynamic model and aerodynamic coefficients written in [12] were used in the simulations. The attitude controller for p, q and r were configured as described in [12]. In the controller, ailerons, elevator and rudder are manipulated variables for each. ARI (ailerons-rudder interconnect), and roll and yaw dumpers are employed. The side-slip angle β is controlled to zero with the rudder.

In all the simulations, design parameters and control gains in all the controllers were kept unchanged, given by

$$\left.\begin{array}{l} \Delta t = 0.1 \text{ s},\ \ t_{\text{aim}} = 4.0 \text{ s},\ \ r_{e_\zeta} = 3.0 \\ t_{\text{ff}} = 1.0 \text{ s},\ \ t_{e_\zeta} = 1.0 \text{ s} \\ K_{\text{aP}} = 0.5,\ \ K_{\text{aI}} = 0,\ \ K_{\text{aD}} = 0.25 \\ \phi_{\text{f}} = 45 \text{ deg},\ \ a_{\text{f}} = 9.0 \text{ m/s}^2 \\ K_{\text{pP}} = 2.0,\ \ K_{\alpha\text{P}} = 3.0,\ \ K_{\alpha\text{I}} = 3.0, \\ \Delta\alpha = 10 \text{ deg}, \end{array}\right\} \quad (26)$$

The ranges for α and a_{z_B} were set, respectively, as $[-5^\circ,\ 20^\circ]$ and [-1 G, 9 G], where 'G' stands for gravity.

Three typical simulation cases and their results will be shown. The desired trajectory for each case is shown below:

Case 1 : Barrel roll (helix about a horizontal axis) –
level flight heading 45 deg from the north for 122 m $\rightarrow$ two rotations of barrel roll of 244 m radius and with the helix angle of 45 deg $\rightarrow$ level flight heading 45 deg from the north (Fig. 7).

Case 2 : Barrel roll of 152 m radius, same as Case 1 except the radius (Fig. 11).

Case 3 : Upward two-quadrant turn and level flight with wind disturbance –
level flight heading north (0 deg) for 122 m $\rightarrow$ a north-upward quadrant of 518 m radius $\rightarrow$ vertical upward for 244 m $\rightarrow$ an upward-east quadrant of 518 m radius $\rightarrow$ (about 16 s from the start) level flight heading east (90 deg) for 122 m; 20 s from the start, step-wise wind disturbance of 30 m/s from the north (Fig. 14).

The desired trajectories above are all smooth. From here, let x, y and z denote the position coordinates of north, west, up directions, respectively, in $\{I\}$ frame. The total simulation time is 40 s for Case 1, and 30 s for Case 2 and 3.

Fig. 7 to Fig. 10 show the result of Case 1. Fig. 7 shows the flight trajectory; Fig. 8 shows the behaviors of position $(x,\ y,\ z)$, velocity V_{a} and yaw angle ψ. Fig. 9 shows the behaviors of angle of attack α, side-slip angle β, pitch rate q and G-force a_{z_B}. Fig. 10 shows the behavior of control inputs: deflections of the ailerons, elevator, rudder (δ_{a}, δ_{e}, δ_{r}) and engine thrust command T_{hc} [%].

In Fig. 8, the position deviation is hardly recognizable and the aircraft flies well along the desired trajectory. The velocity V_{a} drops during upward flight due to the upper limit of T_{hc}, and increases during downward flight.

On the other hand in Fig. 9, α increases close to its upper limit of 20 deg, when the aircraft goes up from the bottom of the barrel. β is kept close to zero. The control inputs in Fig. 10 shows reasonable behaviors.

Next, Figs. 11, 12 and 13 show the result of Case 2, similar to Figs. 7, 8 and 9. In Case 2, the curvature of the desired trajectory is beyond the flight capability. As seen from Fig. 11 to Fig. 12, the position deviation tends to be large during barrel rolls, then decreases close to zero after that. This means that even after the aircraft has gone away from the desired trajectory, it can smoothly come back to the desired trajectory when the desired curvature is within the flight capability. As seen from Fig. 13, α is roughly equal to its upper limit of 20 degrees during barrel rolls, which shows that α limitations work effectively.

And next, Figs. 14 and 15 show the result of Case 3, similar to Figs. 7 and 8. As seen from Figs. 14 and 15, the flight trajectory is well close to the desired one, just like Case 1. V_{a} decreases when the aircraft flies up, and increases to the command V_{ac} when it flies level. Between 13

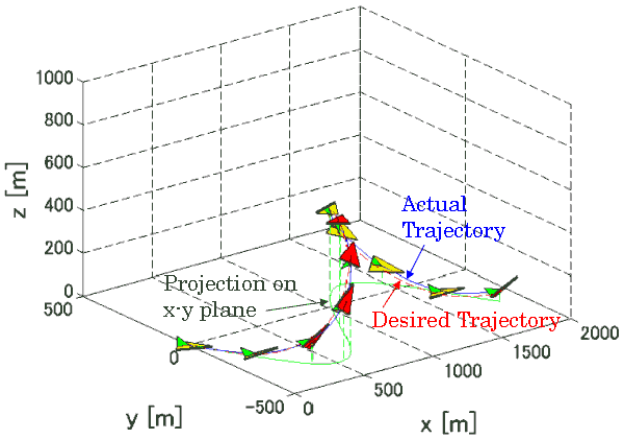

Fig. 7 Case 1: Aircraft Trajectory (first 20 seconds)

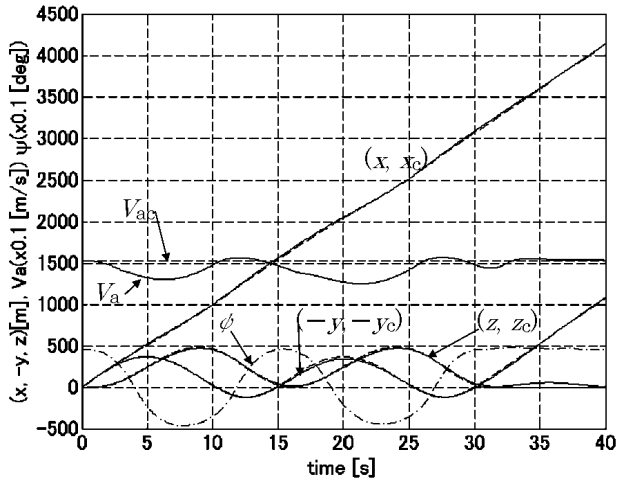

Fig. 8 Case 1: Position, Velocity and Yaw

and 20 seconds from the atart, the yaw angle ψ in Fig. 15 is almost 90 degrees (eastward), the same as the heading angle λ.

After 20 seconds from the start, a step-wise wind disturbance is added, but it hardly disturbs the flight. The yaw angle settles to 78 degrees without changing λ, that is, the aircraft brings its head 12 degrees to the windward to keep its flight direction unchanged.

Thus, as seen from these simulation results, the proposed control works well with various desired trajectories and with wind disturbance. It can bring the aircraft smoothly back to the desired trajectory after the aircraft has flown away from it.

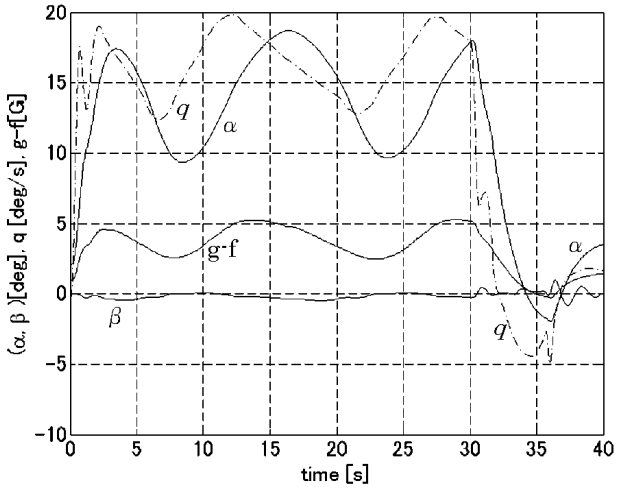

Fig. 9 Case 1: α, β, q and G-force a_{z_B}

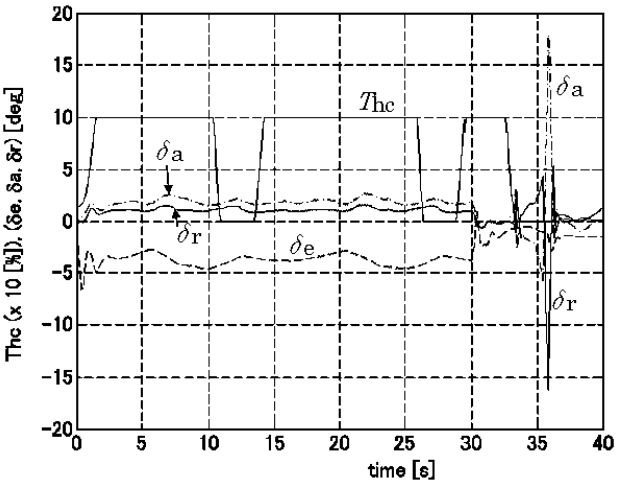

Fig. 10 Case 1: Control Inputs

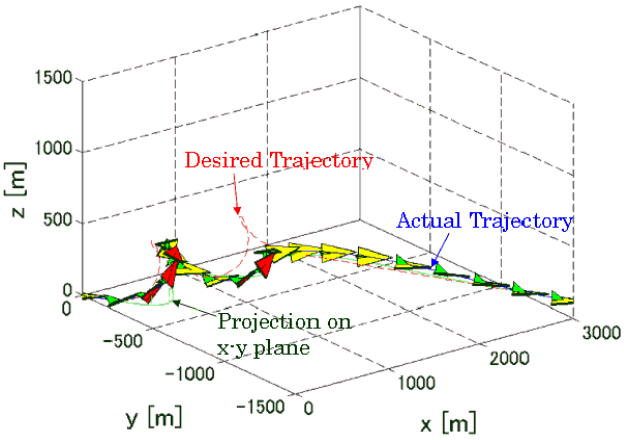

Fig. 11 Case 2: Aircraft Trajectory (30 seconds)

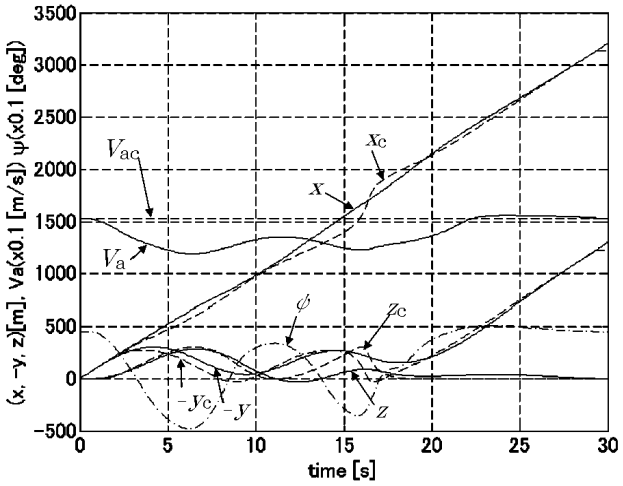

Fig. 12 Case 2: Position, Velocity and Yaw

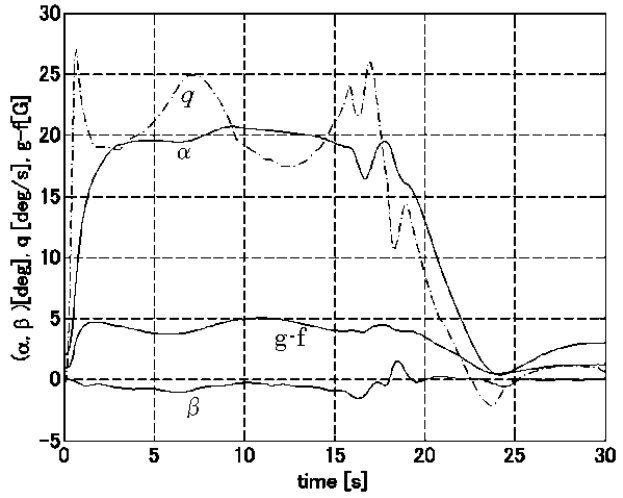

Fig. 13 Case 2: α, β, q and G-force a_{z_B}

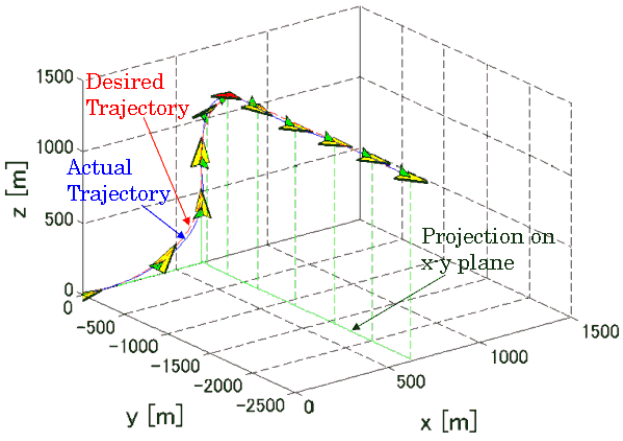

Fig. 14 Case 3: Aircraft Trajectory (30 seconds)

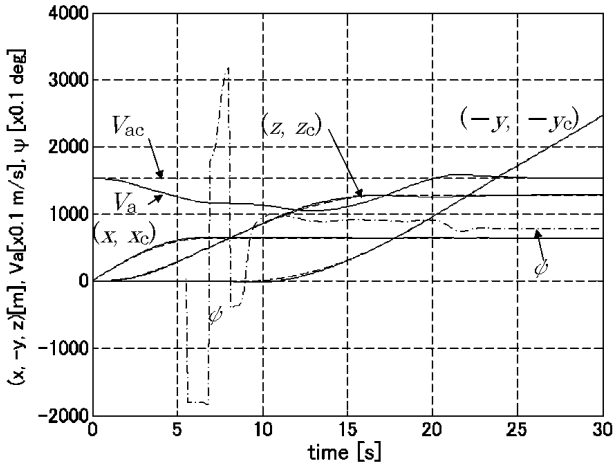

Fig. 15 Case 3: Position, Velocity and Yaw

4 Conclusion

An automatic control of flight trajectory has been presented for fixed-wing aircraft. The proposed control has several features and advantages compared with other studies. The simulation results confirmed the effectiveness of the control.

In the proposed control, it is assumed that measurement values of aircraft position, velocity, direction, attitude and such that can be obtained accurately without time delay, which would be difficult in reality. In actual control, it would be necessary to cope with noises or time delays in measurements. The study on this problem remains for future work.

Acknowledgements

The author would like to express his thankfulness to those members of Fuji Aerospace Technology Co. Ltd. and Fuji Heavy Industries Ltd. who contributed to technical discussions, and those graduates of Teikyo University who contributed to developing the simulation software.

References

[1] Jung Y C and Hess R A. Precise flight-Path control using a predictive algorithm. *J. Guidance*, Vol. 14, No. 5, pp.936-942, 1992.

[2] Steharu-Alexe I and O'Shea J. Four-dimensional guidance of atmospheric vehicles.

J. Guidance, Control and Dynamics, Vol. 19, No. 1, pp.113-122, 1996.

[3] Kaminer I, Pascoal A, Hallberg E and Silvestre C. Trajectory tracking for autonomous vehicles: an integrated approach to guidance and control. *J. Guidance, Control and Dynamics*, Vol. 21, No. 1, pp.29-38, 1998.

[4] Boyle D P and Chamitoff G E. Autonomous maneuver tracking for self-piloted vehicles. *J. Guidance, Control and Dynamics*, Vol. 22, No. 1, pp.58-67, 1999.

[5] Gruszecki J and Pieniążek J. Unmanned aircraft control on the trajectory. *J. of Computer Science and Security*, Vol. 3, No. 2, pp.76-83, 2002.

[6] Takano H and Baba Y. Optimal flight trajectory and acrobatic maneuvers against missiles. *Proc. of the 5th Asian and Control Conference*, Melbourne, Australia, July 20-23, 2004, pp.1841-1848.

[7] Cunha R and Antunes D G. A path-following preview controller for autonomous air vehicles. *Proc. of Guidance, Navigation and Control Conference*, Keystone, CO, 2006.

[8] Sonneveldt L, van Oort E R, Chu Q P and Mulder J A. Nonlinear adaptive trajectory control applied to an F-16 model. *J. Guidance, Control and Dynamics*, Vol. 32, No. 1, pp.25-39, 2009.

[9] Yoshitani N. A heading and flight-Path angle control of aircraft based on required acceleration vector. *Journal of Japan Society of Aeronautics and Space Sciences*, Vol. 52, No. 605, pp.265-271, 2004 (in Japanese).

[10] Yoshitani N. A flight-path control of aircraft based on required acceleration vector. *Journal of Japan Society of Aeronautics and Space Sciences*, Vol. 55, No. 638, pp.111-116, 2007 (in Japanese).

[11] Jennings G A. *Modern geometry with applications*. Springer-Verlag, New York, 1994.

[12] Stevens B L and Lewis F L. *Aircraft control and simulation*. John Wiley & Sons, New York, 1992.

Copyright Statement